Article:
James, A.M. and Dawson, R. orcid.org/0000-0003-4689-4428 (2020) Efficient and tunable white-light emission using a dispersible porous polymer. Macromolecular Rapid Communications, 41 (12). 2000176. ISSN 1022-1336

https://doi.org/10.1002/marc.202000176

Macromolecular Rapid Communication
www.mrc-journal.de

Efficient and Tunable White-Light Emission Using a Dispersible Porous Polymer

*Alex M. James and Robert Dawson**

A dispersible porous polymer (PEG_{113}-*b*-DVB_{800}-*co*-AA_{200}) based on the controlled radical polymerization of divinylbenzene and acrylic acid with a poly(ethylene glycol) (PEG) macrochain transfer agent (macro-CTA) is synthesized and post-synthetically modified with anthracene. This blue-emitting porous polymer is used to encapsulate the yellow-emitting fluorophore rhodamine B into its core, resulting in a white-light emitting dispersion with a quantum yield of 38% and commission internationale de l'éclairage coordinates of ($X = 0.33$, $Y = 0.32$).

Microporous organic polymers (MOPs) are a class of microporous material, which are both chemically and thermally stable (they can be boiled in acid/base without the loss of porosity) and possess high apparent surface areas, some as high as 5000 $m^2\ g^{-1}$.[1–3] Furthermore, they can be tuned toward specific applications such as gas separation[4–6] and storage,[7,8] photocatalysis,[9,10] chemosensing,[11,12] hydrogen evolution,[13–15] and more.[16,17]

One disadvantage of MOPs however is their lack of solubility in common organic solvents due to their extended crosslinked network structure, which ensures their permanent porosity. This lack of solubility hinders the processing of the materials thereby limiting their potential applications despite their many interesting and advantageous properties.[18] There are many subclasses of MOP including conjugated microporous polymers (CMPs)[19,20] and hypercrosslinked polymers (HCPs)[21,22] but only one subclass combines permanent porosity with solubility—polymers of intrinsic microporosity (PIMs).[23,24] The linear yet rigid and contorted structure of PIMs is advantageous to their solution processability, but they too are not without their own drawbacks which includes a limited number of building blocks and a relative lack of functionality compared to other MOPs.

White-light emission from one single material can be difficult to achieve because simultaneous emission of three primary colors to cover the entire visible region of light is needed. As such the vast majority of reports use metal complexes or the complex design of small organic molecules capable of this dual emission.[25,26] Porous materials may offer a unique solution to this problem given that they are capable of encapsulating multiple organic molecules, which could then be used to simultaneously emit light to generating white-light. For this to be realized, it is pivotal that the porous material is also solution processable so it is able to maximize encapsulation of the fluorophores and allow for processing for the desired end application.[27,28]

In recent years, there have been a handful of reports of other soluble porous polymers which use alkyl side chains to aid solubility. In 2012, Cheng et al. reported a soluble conjugated microporous polymer (SCMP-1) with a Brunauer-Emmett-Teller (BET) surface area of 505 $m^2\ g^{-1}$ using *t*-butyl pyrene monomers with a M_n of 4340 g mol^{-1} similar to that of a first generation polyhedral oligomeric silsesquioxane centered pyrene dendrimer.[29] Bandyopadhyay et al. reported another CMP type material this time using a dioctylcyclopentyl monomer, which could be fabricated as a powder, solution and as nanoparticles with a BET surface area of 405 $m^2\ g^{-1}$.[30] Wood and co-workers synthesized the first soluble hypercrosslinked polymers, synthesized by intramolecularly crosslinking individual poly(styrene) chains at high dilution with surface areas ranging from 187 to 724 $m^2\ g^{-1}$.[31] Though these examples of soluble MOPs were found to be both porous and soluble, their synthesis either involved high costs, numerous synthetic steps, or large quantities of carcinogenic solvent. Furthermore, these examples are all very niche and do not provide a generic route to soluble MOPs and hence are unlikely to ever lead to commercial use.

In 2019, we reported the first example of a versatile route to synthesize dispersible microporous polymers via the reversible addition-fragmentation chain-transfer (RAFT) mediated polymerization of divinylbenzene (DVB) and fumaronitrile (FN) using a hydrophilic poly(ethylene glycol) (PEG) macrochain transfer agent (macro-CTA).[32] This was performed in a water/ethanol solvent mixture using a polymerization-induced self-assembly (PISA) approach. The result of this synthesis was a material consisting of a porous core made solution dispersible by the presence of the long hydrophilic outer PEG polymer chains. These porous polymer particles demonstrated long-term stability in a wide variety of different solvents. Our approach has recently been exploited by Ferguson et al. to perform photocatalytic reactions by introducing the crosslinker 4,7-bis(4-vinylphenyl)benzo[*c*][1,2,5]thiadiazole into the cores of the samples during polymerization.[33] This highlights the versatility of the synthetic approach as potentially any vinylic monomer is capable of being polymerized and incorporated into the final product.

Dr. A. M. James, Dr. R. Dawson
Department of Chemistry, Dainton Building
University of Sheffield
Sheffield, South Yorkshire S3 7HF, UK
E-mail: r.dawson@sheffield.ac.uk

The ORCID identification number(s) for the author(s) of this article can be found under https://doi.org/10.1002/marc.202000176.

DOI: 10.1002/marc.202000176

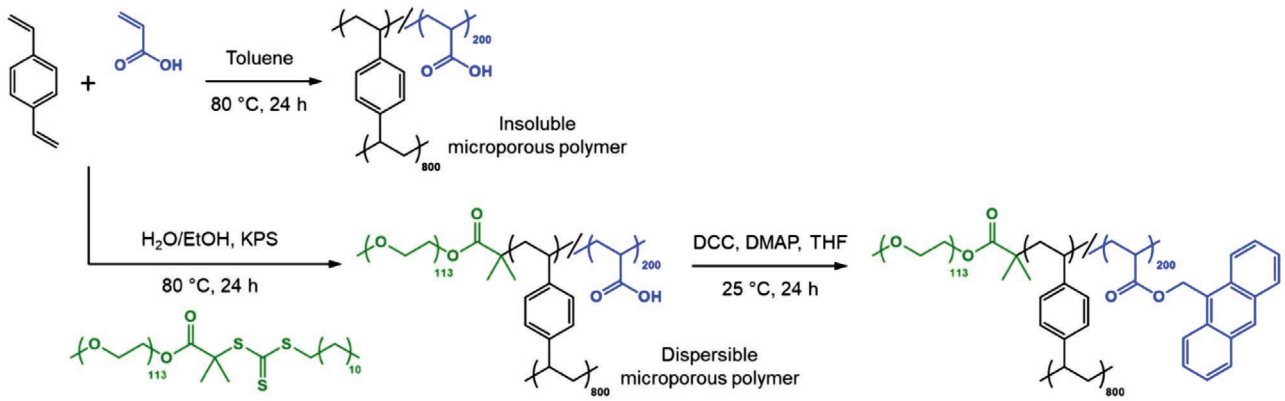

Scheme 1. Synthetic approach utilized to synthesize porous polymer dispersion and the postsynthetic modification.

Building on this work, we now report the synthesis of dispersible microporous polymers to produce white light achieved by post-synthetic modification (PSM) of a DVB and acrylic acid (AA) solution-stable porous dispersion capable of encapsulating the fluorescent dye rhodamine B. Previously, FN was polymerized as a comonomer alongside DVB to produce dispersible microporous polymer particles. Though effective, fumaronitrile cannot be readily functionalized hence further applications or PSM of this material is quite limited. In order to introduce functionality into the core of the particles the use of AA was investigated due to its potential scope for further PSM.

Initially, the synthesis of an insoluble porous material was targeted via conventional free radical polymerization of DVB and AA in toluene (see sections S1 and S4 in the Supporting Information). This reaction resulted in an insoluble porous polymer in good yield (88%) with a BET surface area of 457 m^2 g^{-1} and set the precedence for the synthesis of a dispersible analogue.

As previously reported, the use of a RAFT–PISA approach using a PEG macro-CTA to polymerize DVB alongside a suitable comonomer yields a dispersible microporous polymer (**Scheme 1**).[33] Hence, the same methodology was applied to the synthesis of PEG_{113}-*b*-DVB_{800}-*co*-AA_{200}. PSM of this material was carried out on the acrylic acid functionality embedded into the core of the material using 9-anthracenemethanol via esterification to yield PEG_{113}-*b*-DVB_{800}-*co*-AA/An_{200}.

The solid state ^{13}C cross-polarization magic angle spinning (CP/MAS) NMR spectra of both PEG_{113}-*b*-DVB_{800}-*co*-AA_{200} and PEG_{113}-*b*-DVB_{800}-*co*-AA/An_{200} (Figure 2a) show signals at 13 and 40 ppm due to the presence of $–CH_2–$ and –CH– backbone alkyl carbons indicating that the polymerization of the two monomers was successful. Further resonances in both spectra at 137 ppm are attributed to the quaternary aromatic carbons while those at 128 ppm are attributed to aromatic $C–H_{Ar}$ carbons. The signals at 145 ppm are assigned to the carboxylic acid carbons present due to the successful incorporation of the acrylic acid monomer into the final material. The peak at 113 ppm is due to unreacted vinyl groups most likely present as a result of incomplete polymerization of divinylbenzene. There is a small peak at 70 ppm present in both samples, which highlights the successful inclusion of the PEG macro-CTA into the final product. Unfortunately, due to the small amount of anthracene present in the post-synthetically modified sample, it was not possible to resolve any peaks relating to the inclusion of anthracene aromatic groups in this material. However, it was possible to confirm the presence of anthracene in the modified sample using a combination of UV–vis and fluorescence emission spectroscopy (**Figure 1**). Under UV irradiation, both samples demonstrate fluorescence emission in the UV region between 330 and 350 nm. However, in the case of PEG_{113}-*b*-DVB_{800}-*co*-AA/An_{200}, there are two new peaks present in the blue visible region of light (400–450 nm), which is owed to the incorporation of the anthracene units into the core of the material (Figure 1; Section S6, Supporting Information).

Nitrogen gas adsorption studies were carried out at 77 K, to study the porosity of both samples (**Figure 2**b). Initially, PEG_{113}-*b*-DVB_{800}-*co*-AA_{200} was calculated to have a specific BET surface area of 201 m^2 g^{-1} though after PSM this decreased slightly to 188 m^2 g^{-1} most likely due to the inclusion of some bulky aromatic anthracene units within the porous core of the material. Both materials were found to be lower in surface area than the insoluble analogue, which was also found to be the case for the previously reported divinylbenzene and fumaronitrile analogue.[32] In contrast to the DVB/FN analogue, PEG_{113}-*b*-DVB_{800}-*co*-AA_{200} showed little uptake of gas in the low relative pressure region (<0.1 P/P_0) however incremental uptake was observed over a relative pressure range of 0.2–0.8 P/P_0 indicative of mesoporosity within the materials. This is demonstrated by the pore size distribution analysis (see inset of Figure 2b), which shows a pore size centered around 3 nm, slightly larger than that of a microporous material. Uptake in the high relative pressure range (>0.9 P/P_0) is due to the aggregated morphology observed in the transmission electron microscopy (TEM) (see **Figure 3**a,b) images and similar to that of the DVB/FN analogue. The fact that the surface area has decreased after PSM is indicative of the anthracene units being located within the pores of the material and not merely adsorbed onto the surface of the sample.

Both PEG_{113}-*b*-DVB_{800}-*co*-AA_{200} and PEG_{113}-*b*-DVB_{800}-*co*-AA/An_{200} formed stable dispersions upon sonication in methanol, which allowed for the determination of the particle size via dynamic light scattering (DLS) (Figure 3c). It was expected that the size of the particles would be affected by the solvent as was found for the DVB/FN analogues where the core was shown to swell in good solvents while bad solvents were not able to swell

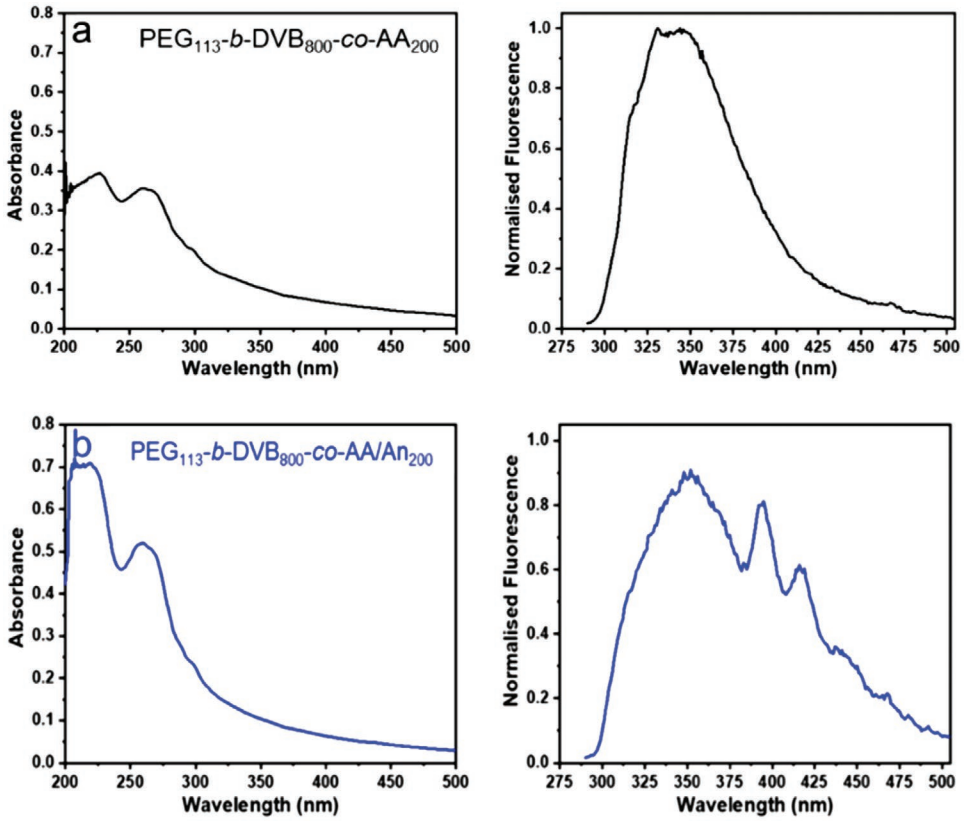

Figure 1. a) (Left) UV–vis absorption spectrum and (right) fluorescence emission spectrum (λ_{max} = 265 nm) of a 0.1 mg mL^{-1} dispersion of PEG_{113}-*b*-DVB_{800}-*co*-AA_{200} in methanol. b) UV–vis absorption spectrum and (right) fluorescence emission spectrum (λ_{max} = 265 nm) of a 0.1 mg mL^{-1} dispersion of PEG_{113}-*b*-DVB_{800}-*co*-AA/An_{200} in methanol.

the core. In PEG_{113}-*b*-DVB_{800}-*co*-AA_{200}, the core is composed of both DVB and AA units whereas in the PEG_{113}-*b*-DVB_{800}-*co*-AA/An_{200} sample a significant proportion of the AA units have been reacted with 9-anthracenemethanol, which alters the solubility of the material. DLS results showed that PEG_{113}-*b*-DVB_{800}-*co*-AA_{200} was indeed larger than PEG_{113}-*b*-DVB_{800}-*co*-AA/An_{200} in methanol with calculated hydrodynamic radii of 1124 and 870 nm, respectively. This is perhaps to be expected given that methanol is a poor solvent for anthracene, which now makes up part of the core of the material.

White light can be generated through the combination of a blue and yellow emitter, which covers most of the visible spectral range (400–800 nm). Being both porous and dispersible, PEG_{113}-*b*-DVB_{800}-*co*-AA/An_{200} can be used to encapsulate organic compounds in solution. Therefore, the yellow emitting organic fluorophore rhodamine B was mixed with a dispersion

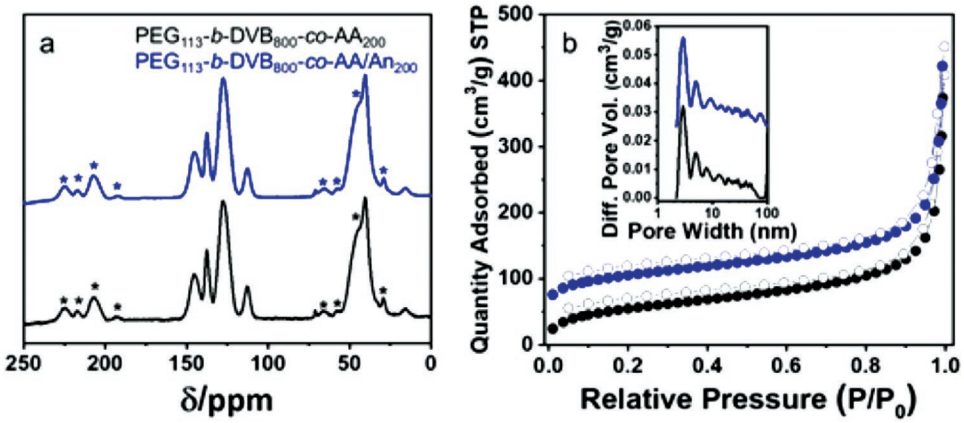

Figure 2. a) ^{13}C CP/MAS NMR and b) N_2 gas sorption isotherms and pore size distribution (inset) of both PEG_{113}-*b*-DVB_{800}-*co*-AA_{200} and PEG_{113}-*b*-DVB_{800}-*co*-AA/An_{200}. Asterisks denote spinning side bands.

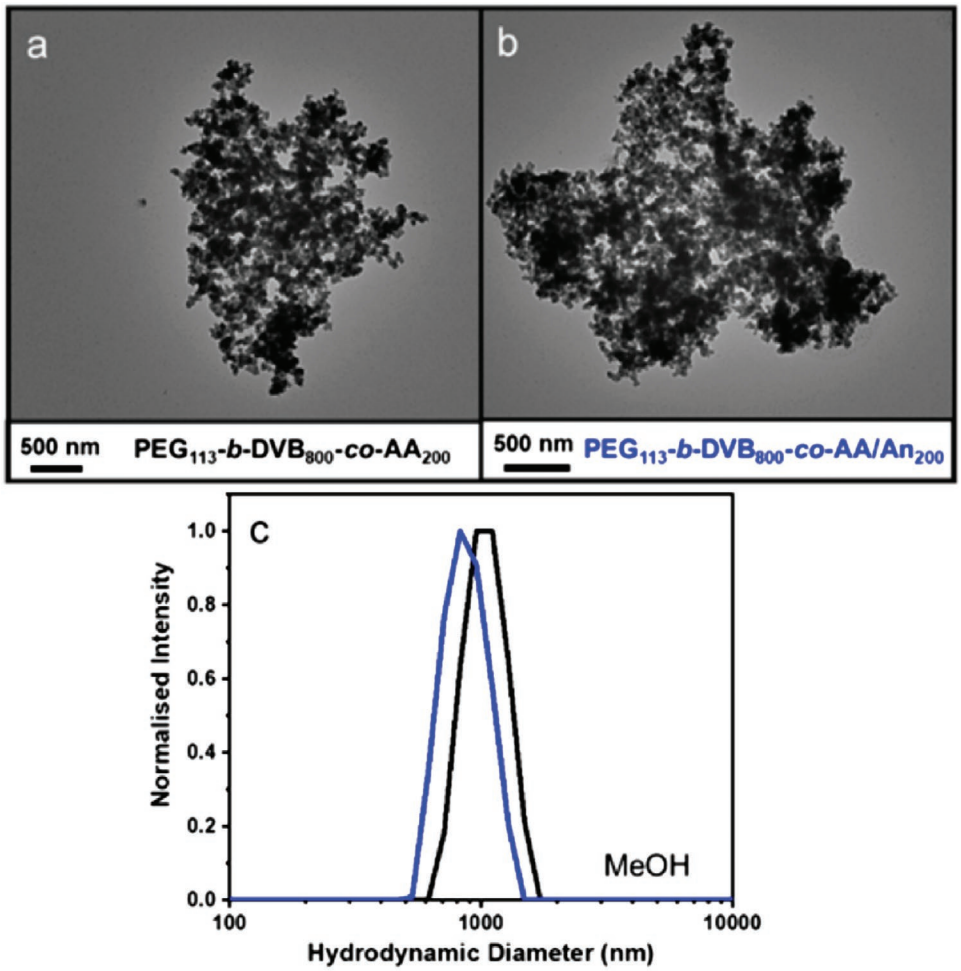

Figure 3. a,b) TEM images and c) DLS curves for both PEG_{113}-*b*-DVB_{800}-*co*-AA_{200} and PEG_{113}-*b*-DVB_{800}-*co*-AA/An_{200} in methanol.

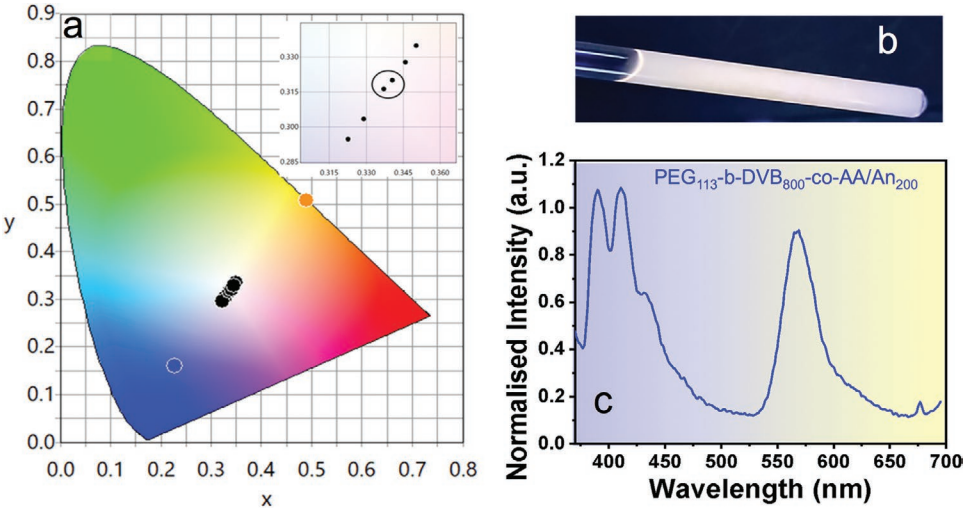

Figure 4. a) CIE plot showing the change in coordinates as more rhodamine B solution is added to the PEG_{113}-*b*-DVB_{800}-*co*-AA/An_{200} dispersion. b) Image of the white-light-emitting solution and fluorescence emission spectrum. c) Normalized fluorescence emission profile of a 1 mg mL^{-1} dispersion of PEG_{113}-*b*-DVB_{800}-*co*-AA/An_{200} and 1.63 ppm of rhodamine B in methanol.

of the blue emitting PEG_{113}-*b*-DVB_{800}-*co*-AA/An_{200} in order to try and generate a white light emitting solution.

Through fine-tuning of the rhodamine B concentration (Section S7, Supporting Information), it was possible to generate a white-light emitting solution upon addition of 1.63 ppm of rhodamine B to a dispersion (1 mg mL^{-1}) of PEG_{113}-*b*-DVB_{800}-*co*-AA/An_{200} (**Figure 4**). Under UV irradiation (λ_{max} = 355 nm) a white-light emitting solution was created with commission internationale de l'éclairage (CIE) coordinates of $X = 0.33$, $Y = 0.32$, close to that of an idealized white light source ($X = 0.33$, $Y = 0.33$). The correlated color temperature (CCT) of the solution was 5239 K, close to that of horizon daylight (5000 K). The quantum yield of this solution was calculated and found to be 38%, which is comparable to most other porous materials that range from 11–38% (see Section S7 in the Supporting Information).

In summary, a porous and solution processable material was synthesized via the controlled radical polymerization of DVB and AA mediated using a PEG-based macro-CTA. Postsynthetic modification of this material using 9-anthracenemethanol resulted in a blue emitting dispersion in which the anthracene is present within the core of the sample. Encapsulation of a yellow emitting fluorophore, rhodamine B, allows for the generation of a white-light emitting solution with CIE coordinates close to that of ideal white light ($X = 0.32$, $Y = 0.32$). The quantum yield of the solution (38%) is comparable to many other porous materials studied for similar applications. This synthetic approach offers the user much scope for modification, which can be exploited when designing processable porous materials for a specific end application. Already this approach has been exploited to design materials capable of chemosensing, photocatalysis, and now white-light emission. In the near future, the group aims to report work on the fabrication of films/membranes from these materials to complement and build on their current uses in solution.

Supporting Information

Supporting Information is available from the Wiley Online Library or from the author.

Conflict of Interest

The authors declare no conflict of interest.

Keywords

microporous polymers, porous dispersible polymers, radical polymerization, solution-processable polymers, white-light emission

Received: March 31, 2020
Revised: May 1, 2020
Published online:

[1] R. Dawson, A. I. Cooper, D. J. Adams, *Prog. Polym. Sci.* **2012**, *37*, 530.
[2] N. Chaoui, M. Trunk, R. Dawson, J. Schmidt, A. Thomas, *Chem. Soc. Rev.* **2017**, *46*, 3302.
[3] D. Yuan, W. Lu, D. Zhao, H. C. Zhou, *Adv. Mater.* **2011**, *23*, 3723.
[4] R. Dawson, L. A. Stevens, T. C. Drage, C. E. Snape, M. W. Smith, D. J. Adams, A. I. Cooper, *J. Am. Chem. Soc.* **2012**, *134*, 10741.
[5] R. T. Woodward, L. A. Stevens, R. Dawson, M. Vijayaraghavan, T. Hasell, I. P. Silverwood, A. V. Ewing, T. Ratvijitvech, J. D. Exley, S. Y. Chong, F. Blanc, D. J. Adams, S. G. Kazarian, C. E. Snape, T. C. Drage, A. I. Cooper, *J. Am. Chem. Soc.* **2014**, *136*, 9028.
[6] R. Dawson, A. I. Cooper, D. J. Adams, *Polym. Int.* **2013**, *62*, 345.
[7] X. Zhu, S. M. Mahurin, S.-H. An, C.-L. Do-Thanh, C. Tian, Y. Li, L. W. Gill, E. W. Hagaman, Z. Bian, J.-H. Zhou, J. Hu, H. Liu, S. Dai, *Chem. Commun.* **2014**, *50*, 7933.
[8] W. Wang, M. Zhou, D. Yuan, *J. Mater. Chem. A* **2017**, *5*, 1334.
[9] P. Pachfule, A. Acharjya, J. Jérô Me Roeser, T. Langenhahn, M. Schwarze, R. Schomä, A. Thomas, J. Schmidt, *J. Am. Chem. Soc.* **2018**, *140*, 1423.
[10] J. X. Jiang, Y. Li, X. Wu, J. Xiao, D. J. Adams, A. I. Cooper, *Macromolecules* **2013**, *46*, 8779.
[11] C. Gu, N. Huang, J. Gao, F. Xu, Y. Xu, D. Jiang, *Angew. Chem., Int. Ed.* **2014**, *53*, 4850.
[12] C. Gu, N. Huang, Y. Wu, H. Xu, D. Jiang, *Angew. Chem., Int. Ed.* **2015**, *54*, 11540.
[13] E. Jin, Z. Lan, Q. Jiang, K. Geng, G. Li, X. Wang, D. Jiang, *Chem* **2019**, *5*, 1632.
[14] Y. Xu, N. Mao, S. Feng, C. Zhang, F. Wang, Y. Chen, J. Zeng, J. X. Jiang, *Macromol. Chem. Phys.* **2017**, *218*, 1700049.
[15] X. Wang, L. Chen, S. Y. Chong, M. A. Little, Y. Wu, W. H. Zhu, R. Clowes, Y. Yan, M. A. Zwijnenburg, R. S. Sprick, A. I. Cooper, *Nat. Chem.* **2018**, *10*, 1180.
[16] C. Wilson, M. Main, N. Cooper, M. E. Briggs, A. I. Cooper, D. Adams, *Polym. Chem.* **2017**, *8*, 1914.
[17] A. M. James, S. Harding, T. Robshaw, N. Bramall, M. D. Ogden, R. Dawson, *ACS Appl. Mater. Interfaces* **2019**, *11*, 22464.
[18] A. G. Slater, A. I. Cooper, *Science* **2015**, *348*, aaa8075.
[19] A. I. Cooper, *Adv. Mater.* **2009**, *21*, 1291.
[20] Y. Xu, S. Jin, H. Xu, A. Nagai, D. Jiang, *Chem. Soc. Rev.* **2013**, *42*, 8012.
[21] L. Tan, B. Tan, *Chem. Soc. Rev.* **2017**, *46*, 3322.
[22] J. Huang, S. R. Turner, *Polym. Rev.* **2018**, *58*, 1.
[23] P. M. Budd, B. S. Ghanem, S. Makhseed, N. B. McKeown, K. J. Msayib, C. E. Tattershall, *Chem. Commun.* **2004**, 230.
[24] N. B. McKeown, *ISRN Mater. Sci.* **2012**, *2012*, 513986.
[25] Y. Yang, T. Wang, P. Yin, W. Yin, S. Zhang, Z. Lei, M. Yang, Y. Ma, W. Duan, H. Ma, *Mater. Chem. Front.* **2019**, *3*, 505.
[26] S. Mukherjee, P. Thilagar, *Dyes Pigm.* **2014**, *110*, 2.
[27] Z. Wang, Z. Wang, B. Lin, X. Hu, Y. Wei, C. Zhang, B. An, C. Wang, W. Lin, *ACS Appl. Mater. Interfaces* **2017**, *9*, 35253.
[28] P. Pallavi, S. Bandyopadhyay, J. Louis, A. Deshmukh, A. Patra, *Chem. Commun.* **2017**, *53*, 1257.
[29] G. Cheng, T. Hasell, A. Trewin, D. J. Adams, A. I. Cooper, *Angew. Chem., Int. Ed.* **2012**, *51*, 12727.
[30] S. Bandyopadhyay, P. Pallavi, A. G. Anil, A. Patra, *Polym. Chem.* **2015**, *6*, 3775.
[31] Y. Yang, B. Tan, C. D. Wood, *J. Mater. Chem. A* **2016**, *4*, 15072.
[32] A. M. James, M. J. Derry, J. S. Train, R. Dawson, *Polym. Chem.* **2019**, *10*, 3879.
[33] C. T. J. Ferguson, N. Huber, T. Kuckhoff, K. A. I. Zhang, K. Landfester, *J. Mater. Chem. A* **2020**, *8*, 1072.